



Article

Theoretical and Experimental Study of the Friction Behavior of Halogen-Free Ionic Liquids in Elastohydrodynamic Regime

Karthik Janardhanan and Patricia Iglesias *

Mechanical Engineering Department, Kate Gleason College of Engineering, Rochester Institute of Technology, Rochester, NY 14623, USA; kj7715@rit.edu

* Correspondence: pxieme@rit.edu; Tel.: +1-585-475-7710

Academic Editors: Antolin Hernández Battez and Rubén González Rodríguez

Received: 31 March 2016; Accepted: 11 May 2016; Published: 19 May 2016

Abstract: Ionic Liquids have emerged as effective lubricants and additives to lubricants, in the last decade. Halogen-free ionic liquids have recently been considered as more environmentally stable than their halogenated counterparts, which tend to form highly toxic and corrosive acids when exposed to moisture. Most of the studies using ionic liquids as lubricants or additives of lubricants have been done experimentally. Due to the complex nature of the lubrication mechanism of these ordered fluids, the development of a theoretical model that predicts the ionic liquid lubrication ability is currently one of the biggest challenges in tribology. In this study, a suitable and existing friction model to describe lubricating ability of ionic liquids in the elastohydrodynamic lubrication regime is identified and compared to experimental results. Two phosphonium-based, halogen-free ionic liquids are studied as additives to a Polyalphaolefin base oil in steel–steel contacts using a ball-on-flat reciprocating tribometer. Experimental conditions (speed, load and roughness) are selected to ensure that operations are carried out in the elastohydrodynamic regime. Wear volume was also calculated for tests at high speed. A good agreement was found between the model and the experimental results when [THTDP][Phos] was used as an additive to the base oil, but some divergence was noticed when [THTDP][DCN] was added, particularly at the highest speed studied. A significant decrease in the steel disks wear volume is observed when 2.5 wt. % of the two ionic liquids were added to the base lubricant.

Keywords: ionic liquids; halogen-free; friction; elastohydrodynamic; wear

1. Introduction

Almost all of the machines that we use today run on some source of energy. However, a fair amount of this energy is lost as frictional force has to be overcome. Moreover, wearing out of the contact surfaces is responsible for a large amount of mechanical failures. Lubricants are important fluids as they are responsible for reducing friction, removal of wear particles and, hence, minimizing loss of energy [1]. In the transportation industry, overcoming friction is one of the main focus areas as, in passenger cars for example, almost one third of the total energy is used to overcome friction in the tires, brakes, transmission and the engine [2]. It is estimated, that between 1% and 1.55% of a country's Gross Domestic Product (GDP) can be saved if friction and wear losses in mechanical parts were reduced. It is also estimated that approximately 11% of the total energy consumed in the U.S. annually in the areas of transportation, turbomachinery, power generation, and industrial processes can be saved through new developments in lubrication and tribology [3].

In the last decade, Ionic Liquids (ILs) have emerged as high performance fluids due to their unique characteristics [4,5]. Their high thermal stability, low vapor pressure, non-flammability,

non-volatility, high viscosity, broad liquid range, high ionic conductivity, wide electrochemical window, and miscibility with organic compounds make them ideal candidates for many engineering applications. ILs are salts with melting points lower than 100 °C; and are usually composed of an organic cation and a weakly coordinating anion. Besides the above-mentioned properties, ILs have the ability to form highly ordered adsorbed layers [6,7] on metal surfaces reducing friction and wear of mechanical components. The use of ILs as neat lubricants was first reported in 2001 [7]. Since then, ILs have emerged as promising advanced lubricants, not only as neat oils [8,9], but also as lubricant additives [9–11]. Another reason behind choosing ILs as our lubricant is the fact that they can be considered as green substances when they are free of halogens [12]. Experimental studies using halogen-free ILs have provided favorable results in the past [13,14]. This is a major advantage that these liquids hold over all the various commercially available lubricants.

In the past, ILs have primarily been studied in the boundary lubrication regime [4,15] and more information about their behavior in the elastohydrodynamic regime is required. This study will focus on the elastohydrodynamic lubrication regime and a friction model based on this regime will be used to compare experimental results so as to narrow down requirements for an acceptable lubrication mechanism model. The tribological behavior of two phosphonium-based ILs, Tetradecyltrihexylphosphonium bis(2,4,4-trimethylpentyl)phosphinate [THTDP][Phos] and Trihexyltetradecylphosphonium Decanoate [THTDP][DCN], is investigated as additives of a synthetic polyalphaolefin oil—Synton PAO-40 (PAO)—in steel–steel contact. PAO-IL blends containing between 0.5% wt. to 2.5% wt. of each IL are investigated using a block-on-flat reciprocating tribometer and the experimental results are compared to the results obtained from an existing elastohydrodynamic friction model.

2. Theory

2.1. Friction in Elastohydrodynamic Contacts

Elastohydrodynamic Lubrication (also referred to as EHD) is a form of hydrodynamic lubrication wherein the existence of a fluid film between two contacts is explained by the elastic deformation of the surfaces under very high pressures and also the change in the viscosity of the fluid with pressure [16,17]. Various rheological models for evaluating the friction coefficient in the EHD regime exist. The approach used in this study is to determine the shear stress using one of these models. The shear stress is then integrated over the contact area to determine the friction force and thereby the coefficient of friction [18]. Based on the load, elasticity of the materials and sliding speed planned, the regime of lubrication can be set. In this study, the elastohydrodynamic regime will be used. Using the chart of Hamrock and Dowson, Otero *et al.* [19] selected the following correlation to calculate the central film thickness:

$$h_c = 1.39 \left(\frac{\eta_0 U}{2E^* R} \right)^{0.67} (\alpha E^*)^{0.53} \left(\frac{E^* R^2}{W} \right)^{0.067} \quad (1)$$

It should be noted that Equation (1) is valid for unidirectional motion for reciprocating motion when large stroke lengths are applied [20]. Once the film thickness is known, the film parameter (λ) is used to determine the lubrication regime. If the film parameter is between 3 and 10, elastohydrodynamic regime can be considered [19]. Given the surface roughness of the two mating surfaces (σ_1, σ_2), the film parameter is given by:

$$\lambda = \frac{h_c}{\sqrt{\sigma_1^2 + \sigma_2^2}} \quad (2)$$

The rheological model considered under this study is Carreau Model [19]. A generalized viscosity formula is provided by:

$$\frac{\eta}{\eta_0 e^{\alpha p}} = \left[1 + \left(\frac{\eta_0 e^{\alpha p} \Delta U}{G} \right)^2 \right]^{\frac{n-1}{2}} \quad (3)$$

where exponent n and shear modulus G are lubricant specific properties obtained by curve fits to data. The calculation of the Barus pressure viscosity coefficient (α) is explained in Section 2.2.

In a Newtonian fluid, the shear stress is given by,

$$\tau = \frac{\eta e^{\alpha p} \Delta U}{h_c} \quad (4)$$

where the viscosity is given by Equation (3). The friction force is then obtained by integrating the shear stress over the contact area. Dividing the friction force by the normal load, the coefficient of friction is determined. The expression for the friction coefficient is given by:

$$\mu = 3 \left(\frac{\eta_0 \Delta U}{h_c} \right)^n G^{1-n} (e^{n\alpha p_0} [n\alpha p_0 - 1] + 1) \frac{1}{(n\alpha)^2 p_0^3} \quad (5)$$

Here p_0 is the Hertz pressure for a point contact [19] given by:

$$p_0 = \frac{3W}{2\pi a^2} \quad (6)$$

2.2. Calculating the Barus and Roelands Pressure Viscosity Coefficient (α)

The pressure viscosity coefficient of most ionic liquids has not been documented. Pensado *et al.* [21] have determined this coefficient for a few imidazolium based ionic liquids using already published data [22–24]. As the viscosity pressure data for the ionic liquids and the mixtures of ionic liquids used in this study are unavailable, an alternative method has been used.

The Barus (Equation (7)) and Roelands (Equation (8)) pressure viscosity relations are presented below:

$$\eta_p = \eta_0 e^{\alpha p} \quad (7)$$

$$\eta = \eta_0 e^{\left\{ \ln\left(\frac{\eta_0}{\eta_R}\right) \left[\left(1 + \frac{p}{p_r}\right) Z - 1 \right] \right\}} \quad (8)$$

where, η_R and p_r are reference viscosity and pressure ($\eta_R = 6.315 \times 10^{-5}$ Pa·s and $p_r = 1.98 \times 10^8$ Pa), α is the Barus Pressure-Viscosity Coefficient, and Z is Roelands' Pressure Viscosity index.

The Roeland pressure viscosity index can be approximated from the relation given by Fein and Roelands [25,26].

$$Z = [7.81 (H_{40} - H_{100})]^{1.5} F_{40} \quad (9)$$

where

$$F_{40} = (0.885 - 0.864H_{40}); H_{40} = \log(\log(\eta_{40}) + 1.200); H_{100} = \log(\log(\eta_{100}) + 1.200) \quad (10)$$

and η_{40} and η_{100} are the viscosities of the liquid at 40 °C and 100 °C respectively.

The above correlation gives good estimates for synthetic hydrocarbons, polymers, diesters, polyolesters, and hydrocarbon and ester-base oils with additives [25]. This is applicable to this work as the base lubricant is a synthetic hydrocarbon.

If we assume that at ambient pressure ($p = 0$), the slopes of the Barus and Roelands equation are equal, then the Barus parameter can be obtained from the Roelands one using [27]:

$$\alpha = \frac{Z \ln\left(\frac{\eta_0}{\eta_r}\right)}{p_r} \quad (11)$$

Moes [28] showed that the reciprocal asymptotic isoviscous pressure coefficient, α^* , provides a better solution when compared to α . The authors in [28], also provided the following correlation between α and α^* , that is used in this study:

$$\alpha^* \approx \frac{\alpha}{1 + ((1 - Z)(\alpha p_r))} \quad (12)$$

The results of the above calculations can be found below.

3. Experimental Details

3.1. Lubricants

The base lubricant for this study is Synton PAO-40 (PAO) a synthetic oil. Two ionic liquids are used as additives to the base lubricant. The ionic liquids used were obtained commercially from Sigma-Aldrich (USA). Their details are presented in Table 1.

Table 1. Name and structure of ILs used in this study.

Code	Structure		IUPAC Name
	Cation	Anion	
[THTDP][DCN]			Trihexyltetradecylphosphonium decanoate
[THTDP][Phos]			Trihexyltetradecylphosphonium bis(2,4,4-trimethylpentyl)phosphinate

3.2. Tribological Experiments

AISI 52100 steel flat disks (19 mm diameter, 62 hardness HRC, Roughness Ra = 0.1–0.4 μm) were tested in a ball-on-flat reciprocating tribometer against AISI 420C steel balls (1.5 mm spherical diameter, 55–58 hardness HRC, Roughness Ra = 0.05 μm). Tribological tests were carried out at room temperature and under a normal load of 5 N (2.75 GPa maximum Hertzian pressure), and three different speeds of 0.01 m/s, 0.02 m/s and 0.04 m/s. The roughness was varied according to the speed to ensure that the film parameter (λ) was always between 3 and 10, thereby ensuring we were operating in the elastohydrodynamic regime. Table 2 shows the values of roughness used at different speeds and the calculated film parameter using Equation (2). As the film parameter is always between 3 and 10, we ensure that we are operating in the elastohydrodynamic regime.

Table 2. Roughness values at each speed.

Speed (m/s)	Roughness (μm)	Film Parameter (λ)
0.01	0.10	6.29
0.02	0.20	6.82
0.04	0.40	6.98

Friction coefficients were continuously recorded with sliding distance. Mean friction coefficients and wear volume were obtained after three tests under the same conditions. Volume loss (V_f) was determined by image analysis after 45 wear track width (W_t) measurements for each test, according to Equation (13) [29]:

$$V_f = L_s \left[R_f^2 * \sin^{-1} \left(\frac{W_t}{2 * R_f} \right) - \left(\frac{W_t}{2} \right) \left(\frac{R_f}{h_f} \right) \right] + \frac{\pi}{3} (3R_f - h_f) \quad (13)$$

where L_s is stroke length, R_f is the radius of 420C steel ball and h_f is the wear depth given by Equation (14)

$$h_f = R_f - \sqrt{R_f^2 - \frac{W_t^2}{4}} \quad (14)$$

3.3. Viscosity of Lubricants

Viscosities at 40 °C and 100 °C were obtained using a Brookfield DV II+ viscometer with a small sample attachment. The results are presented in Table 3.

Table 3. Viscosity and pressure viscosity coefficient of the lubricants.

Lubricant	Viscosity (cP)		Pressure Viscosity Coefficient α^* (GPa ⁻¹)
	40 °C	100 °C	
PAO	325.00	32.00	16.38
PAO + 0.5% [THTDP][Phos]	330.09	32.34	16.39
PAO + 2.5% [THTDP][Phos]	331.99	32.13	16.55
PAO + 0.5% [THTDP][DCN]	339.00	32.70	16.51
PAO + 2.5% [THTDP][DCN]	343.30	30.85	17.56

4. Results and Discussion

4.1. Viscosities and Pressure Viscosity Coefficients of Lubricants

The viscosities at 40 °C and 100 °C along with the pressure viscosity coefficient at 40 °C are listed in Table 3. The addition of the ionic liquids increased the viscosity of the PAO slightly.

4.2. Friction

Figures 1–3 compare the friction coefficients obtained from the experiments and Carreau model at different sliding speeds. From the figures, the addition of the ILs or increasing sliding speed have no significant effect on the friction values obtained both experimentally and theoretically.

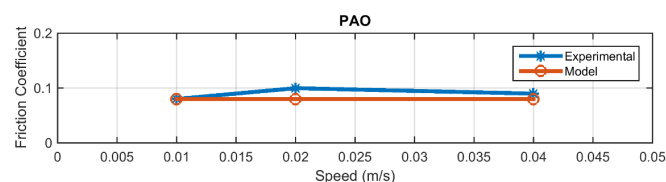


Figure 1. Comparison of Experimental results to theoretical model using PAO.

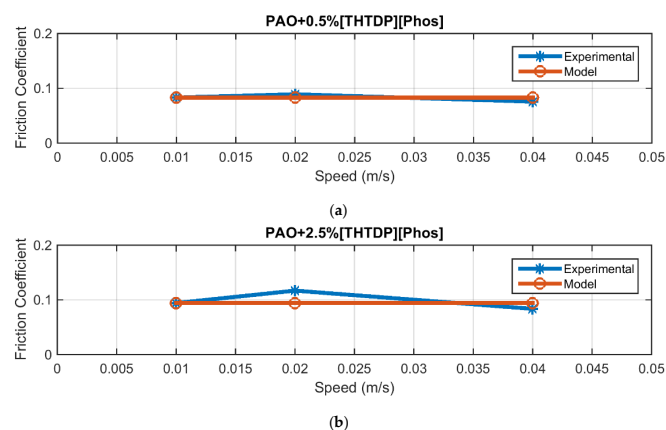


Figure 2. Comparison of Experimental results to theoretical model using (a) 0.5% [THTDP][Phos]; and (b) 2.5% [THTDP][Phos] as an additive to PAO.

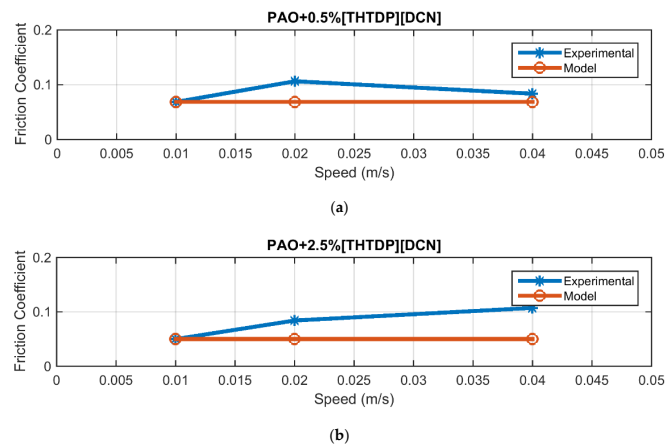


Figure 3. Comparison of Experimental results to theoretical model using (a) 0.5% [THTDP][DCN]; and (b) 2.5% [THTDP][DCN] as an additive to PAO.

Table 4 shows the RMS (Root mean square) error values between the experimental results and the model.

Table 4. RMS Error values between the experimental results and the model.

Lubricant	RMS Error
PAO	0.0110
PAO + 0.5% Phos	0.0048
PAO + 2.5% Phos	0.0125
PAO + 0.5% DCN	0.0203
PAO + 2.5% DCN	0.0333

As expected, a good agreement between the theoretical and experimental results is found when PAO is used as lubricant (Figure 1). The addition of [THTDP][Phos] does not impact the accuracy of the model (Figure 2) as evidenced by the RMS values. When [THTDP][DCN] is used as additive of PAO (Figure 3), a higher difference between the model and experimental results is observed, particularly as the concentration of this IL and sliding speed of the tests is increased. It is well known that ILs have the ability to form highly ordered absorbed layers [6,9,30] that reduce friction and wear of the materials in contact [31,32]. The formation of this tribofilm is favored by the polarity of the anion and high values of pressure and/or speed. The higher deviation between the model and experimental results when the concentration of [THTDP][DCN] and sliding speed increase, may be due to tribochemical reactions of the IL to form the ordered layer on the metallic surfaces [33]; and such a phenomenon is unaccounted in the model used in this study.

4.3. Wear

Figure 4 shows the wear volumes of steel disks after the tests under the fastest speed (0.04 m/s) used in this study. As can be seen, an important reduction of the disk wear volumes is observed when the highest concentration of [THTDP][Phos] and for both concentrations of [THTDP][DCN] are used as additives. This reduction is particularly important when 2.5 wt. % of [THTDP][DCN] is used, where a wear reduction of 80% is observed compared to the PAO. This decrease in wear further supports the formation of a tribolayer at this speed and concentration of [THTDP][DCN].

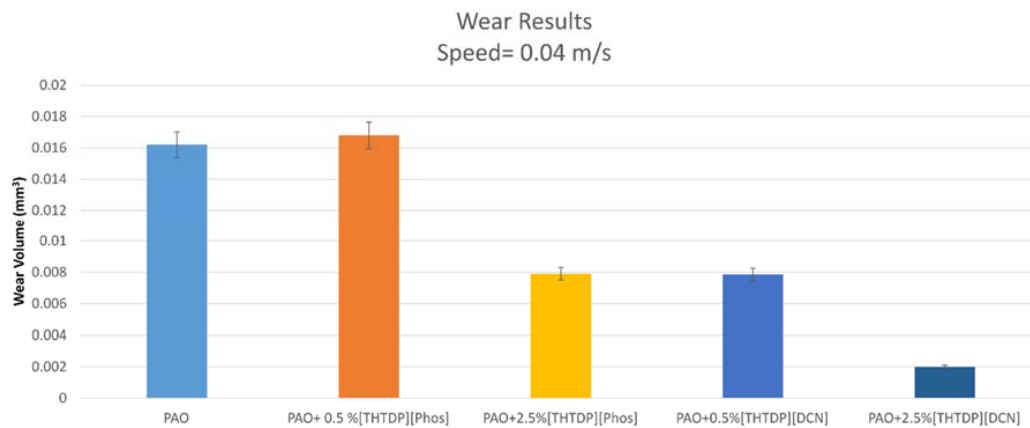


Figure 4. Wear volume of steel disks after a test at 0.04 m/s.

Figure 5 shows the optical micrographs of the steel worn surfaces after a test at 0.04 m/s and lubricated with PAO, PAO + 2.5% [THTDP][Phos] and PAO + 2.5% [THTDP][DCN]. From the figure, wear tracks when ILs are used as additives of PAO are not only narrower but more superficial and smoother than the wear track obtained after a test with PAO. In addition, extensive plastic deformation and fatigue crack propagation are observed when ILs are not present in the base oil.

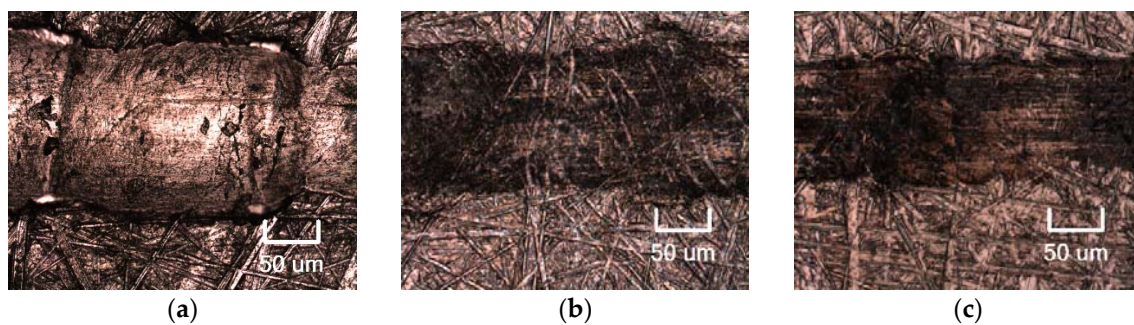


Figure 5. Optical micrographs of wear scars on steel disks after a test at 0.04 m/s and lubricated with: (a) PAO; (b) PAO + 2.5% [THTDP][Phos]; and (c) PAO + 2.5% [THTDP][DCN].

5. Conclusions

This paper studies the tribological effects of the addition of two halogen-free ionic liquids to a synthetic oil in steel–steel contact using a ball-on-flat reciprocating tribometer. The experimental friction results are compared to those obtained using an existing elastohydrodynamic friction model. Experimental conditions (speed, load and roughness) are selected to ensure that operations are carried out in the elastohydrodynamic regime.

The addition of the ILs showed a slight increase in both the viscosity and the pressure-viscosity coefficient of the PAO. A good agreement was found between the model and the experimental results when [THTDP][Phos] was used as an additive to the base oil but some divergence was noticed when [THTDP][DCN] was added, particularly at the highest speed studied. This higher deviation may be due to tribochemical reactions of the IL to form the ordered layer on the metallic surfaces. A significant decrease in the steel disks wear volume is observed when 2.5 wt. % of the two ionic liquids are added to the base lubricant.

Acknowledgments: The authors wish to thank the financial support of the Mechanical Engineering Department at Kate Gleason College of Engineering of the Rochester Institute of Technology.

Author Contributions: Karthik Janardhanan performed the experiments under the supervision of Patricia Iglesias. All authors contributed equally to the design of the experiments and analysis of the data. Karthik Janardhanan wrote the paper with cooperation of Patricia Iglesias.

Conflicts of Interest: The authors declare no conflict of interest.

Appendix

List of symbols

a	Cylinder Diameter (meters)
α	Barus Pressure-Viscosity Coefficient (GPa^{-1})
α^*	Bloks Reciprocal Isoviscous Pressure Coefficient (GPa^{-1})
η	Viscosity (cP)
p	Pressure (MPa)
Z	Roeland's Pressure-Viscosity Index
h	Film Thickness (m)
U	Speed (m/s)
E^*	Young's Reduced Modulus (GPa)
R	Reduced Radius of Curvature (m)
λ	Film Parameter
σ	Surface Roughness (μm)
τ	Shear Stress (N/m^2)
μ	Coefficient of Friction
G	Shear Modulus (Gpa)

References

1. Sripada, P.K.; Sharma, R.V.; Dalai, A.K. Comparative study of tribological properties of trimethylolpropane-based biolubricants derived from methyl oleate and canola biodiesel. *Ind. Crops Prod.* **2013**, *50*, 95–103. [[CrossRef](#)]
2. Holmberg, K.; Andersson, P.; Erdemir, A. Global energy consumption due to friction in passenger cars. *Tribol. Int.* **2012**, *47*, 221–234. [[CrossRef](#)]
3. Tzanakis, I.; Hadfield, M.; Thomas, B.; Noya, S.M.; Henshaw, I.; Austen, S. Future perspectives on sustainable tribology. *Renew. Sustain. Energy Rev.* **2012**, *16*, 4126–4140. [[CrossRef](#)]
4. Zhou, F.; Liang, Y.; Liu, W. Ionic liquid lubricants: Designed chemistry for engineering applications. *Chem. Soc. Rev.* **2009**, *38*, 2590–2599. [[CrossRef](#)] [[PubMed](#)]
5. Bermúdez, M.D.; Jiménez, A.E.; Sanes, J.; Carrión, F.J. Ionic liquids as advanced lubricant fluids. *Molecules* **2009**, *14*, 2888–2908. [[CrossRef](#)] [[PubMed](#)]
6. Minami, I. Ionic liquids in tribology. *Molecules* **2009**, *14*, 2286–2305. [[CrossRef](#)] [[PubMed](#)]
7. Ye, C.; Liu, W.; Chen, Y.; Yu, L. Room-temperature ionic liquids: A novel versatile lubricant. *Chem. Commun. (Camb.)* **2001**. [[CrossRef](#)]
8. Totolin, V.; Minami, I.; Gabler, C.; Dörr, N. Halogen-free borate ionic liquids as novel lubricants for tribological applications. *Tribol. Int.* **2013**, *67*, 191–198. [[CrossRef](#)]
9. Jiménez, A.E.; Bermúdez, M.D.; Iglesias, P.; Carrión, F.J.; Martínez-Nicolás, G. 1-N-alkyl-3-methylimidazolium ionic liquids as neat lubricants and lubricant additives in steel-aluminium contacts. *Wear* **2006**, *260*, 766–782. [[CrossRef](#)]
10. Jiménez, A.E.; Bermúdez, M.D. Ionic liquids as lubricants of titanium-steel contact. *Tribol. Lett.* **2009**, *33*, 111–126. [[CrossRef](#)]
11. Grace, J.; Vysochanska, S.; Lodge, J.; Iglesias, P. Ionic Liquids as Additives of Coffee Bean Oil in Steel-Steel Contacts. *Lubricants* **2015**, *3*, 637–649. [[CrossRef](#)]
12. Song, Z.; Liang, Y.; Fan, M.; Zhou, F.; Liu, W. Ionic liquids from amino acids: Fully green fluid lubricants for various surface contacts. *RSC Adv.* **2014**, *4*, 19396–19402. [[CrossRef](#)]

13. Espinosa, T.; Jimenez, M.; Sanes, J.; Jimenez, A.E.; Iglesias, M.; Bermudez, M.D. Ultra-low friction with a protic ionic liquid boundary film at the water-lubricated sapphire-stainless steel interface. *Tribol. Lett.* **2014**, *53*, 1–9. [[CrossRef](#)]
14. Espinosa, T.; Sanes, J.; Jiménez, A.E.; Bermúdez, M.D. Protic ammonium carboxylate ionic liquid lubricants of OFHC copper. *Wear* **2013**, *303*, 495–509. [[CrossRef](#)]
15. Kondo, Y.; Koyama, T.; Sasaki, S. Tribological Properties of Ionic Liquids. In *Ionic Liquids—New Aspects for the Future*; Intech: Rijeka, Croatia, 2013.
16. Jacod, B. Friction in Elasto-Hydrodynamic Lubrication. Ph.D. Thesis, University of Twente, Twente, The Netherlands, 2002.
17. Stachowiak, G.; Batchelor, A.W. *Engineering Tribology*, 3rd ed.; Butterworth-Heinemann: Burlington, MA, USA, 2005.
18. Spikes, H.; Jie, Z. History, Origins and Prediction of Elasto-hydrodynamic Friction. *Tribol. Lett.* **2014**, *56*, 1–25. [[CrossRef](#)]
19. Otero, J.E.; Morgado, P.L.; Sánchez-Peñuela, J.B.; Sanz, J.L.M.; Muñoz-Guijosa, J.M.; Lantada, A.D.; Yustos, H.L. Elasto-hydrodynamic Models for Predicting Friction in Point Contacts Lubricated with Polyalphaolefins. In *Proceedings of EUCOMES 08 SE—27*; Ceccarelli, M., Ed.; Springer: Dordrecht, The Netherlands, 2009; pp. 219–227.
20. Nishikawa, H.; Handa, K.; Kaneta, M. Behavior of EHL Films in Reciprocating Motion. *Trans. Jpn. Soc. Mech. Eng. Ser. C* **1992**, *58*, 1911–1918. [[CrossRef](#)]
21. Pensado, A.S.; Comuñas, M.J.P.; Fernández, J. The pressure-viscosity coefficient of several ionic liquids. *Tribol. Lett.* **2008**, *31*, 107–118. [[CrossRef](#)]
22. Harris, K.R.; Woolf, L.A.; Kanakubo, M. Temperature and Pressure Dependence of the Viscosity of the Ionic Liquid 1-Butyl-3-methylimidazolium Hexafluorophosphate. *J. Chem. Eng. Data* **2005**, *50*, 1777–1782. [[CrossRef](#)]
23. Harris, K.R.; Kanakubo, M.; Woolf, L.A. Temperature and pressure dependence of the viscosity of the ionic liquids 1-hexyl-3-methylimidazolium hexafluorophosphate and 1-butyl-3-methylimidazolium Bis(trifluoromethylsulfonyl)imide. *J. Chem. Eng. Data* **2007**, *52*, 1080–1085. [[CrossRef](#)]
24. Harris, L.K.R.; Kanakubo, M.; Woolf, A.; Data, J.C.E. Temperature and Pressure Dependence of the Viscosity of the Ionic Liquid 1-Butyl-3-methylimidazolium Tetrafluoroborate: Viscosity and Density Relationships in Ionic Liquids. *J. Chem. Eng. Data* **2007**, *52*, 2425–2430. [[CrossRef](#)]
25. Fein, R. High Pressure Viscosity and EHL Pressure-Viscosity Coefficients. In *Tribology Data Handbook*; CRC Press: Boca Raton, USA, 1997.
26. Roelands, C. Correlational Aspects of the Viscosity-Temperature Pressure Relationship of Lubricating Oils. Ph.D. Thesis, Delft Institute of Technology, Groningen, The Netherlands, 1966.
27. Leeuwen, H. The determination of the pressure–viscosity coefficient of a lubricant through an accurate film thickness formula and accurate film thickness measurements. *J. Eng. Tribol.* **2009**, *223*, 1143–1163. [[CrossRef](#)]
28. Moes, H. *Lubrication and Beyond*; Utwente Lect. Notes; Twente University Press: Enschede, The Netherlands, 2000; Volume 366.
29. Qu, J.; Truhan, J.J. An efficient method for accurately determining wear volumes of sliders with non-flat wear scars and compound curvatures. *Wear* **2006**, *261*, 848–855. [[CrossRef](#)]
30. Somers, A.; Howlett, P.; MacFarlane, D.; Forsyth, M. A Review of Ionic Liquid Lubricants. *Lubricants* **2013**, *1*, 3–21. [[CrossRef](#)]
31. Jiménez, A.E.; Bermúdez, M.D.; Iglesias, P. Lubrication of Inconel 600 with ionic liquids at high temperature. *Tribol. Int.* **2009**, *42*, 1744–1751. [[CrossRef](#)]
32. Iglesias, P.; Bermúdez, M.D.; Carrión, F.J.; Martínez-Nicolás, G. Friction and wear of aluminium-steel contacts lubricated with ordered fluids-neutral and ionic liquid crystals as oil additives. *Wear* **2004**, *256*, 386–392. [[CrossRef](#)]
33. Palacio, M.; Bhushan, B. A review of ionic liquids for green molecular lubrication in nanotechnology. *Tribol. Lett.* **2010**, *40*, 247–268. [[CrossRef](#)]

